

**N-TERMINAL TRUNCATION OF PHA
SYNTHASE (PHAC_{BP-M-CPF4}) AS A STRATEGY
FOR IMPROVED POLYHYDROXYALKANOATE
PROPERTIES BY Cupriavidus necator**

NEOH SOON ZHER

UNIVERSITI SAINS MALAYSIA

2025

**N-TERMINAL TRUNCATION OF PHA
SYNTHASE (PHAC_{BP-M-CPF4}) AS A STRATEGY
FOR IMPROVED POLYHYDROXYALKANOATE
PROPERTIES BY Cupriavidus necator**

by

NEOH SOON ZHER

**Thesis submitted in fulfillment of the requirements
for the degree of
Doctor of Philosophy**

January 2025

ACKNOWLEDGEMENT

Firstly, I am eternally grateful and thankful to the almighty God and the higher powers for their blessings throughout this project; thank you for enlightening and guiding me towards the right path.

I wish to also express my greatest and sincerest gratitude to my supervisor Professor Dr. K. Sudesh Kumar for his endless guidance, motivation, and advice throughout this project. His dedication and passion as an educator and a supervisor are indeed very inspiring and sparked my interest in biotechnology.

Next, I would also like to thank my seniors, Dr. Tan Hua Tiang and Ms. Ang Shaik Ling for their help, advice, and camaraderie. My deepest gratitude also goes to my fellow labmates: Mr. Thinagaran, Ms. Chanaporn Trakunjae, Ms. Tang Hui Jia, Ms. Wan Jia Hui, Ms. Amirah, Ms. Aishu, and Ms. Shahira for their constant support and friendship. Their presence in Lab 409 filled my journey throughout my project with warmth and comfort.

I also wish to extend my thanks to Dr. Chek Min Fey from NAIST for his guidance throughout my study. I would also like to thank the lab assistants from the electron microscope unit and microbiology lab for their endless help and support at crucial moments. My gratitude also goes to those who helped me indirectly upon completing my study. I would like to thank Ms. Neoh Way Sze for her English proofreading.

Lastly, I wish to also express my deepest gratitude to my parents, family, and friends for their unconditioned support and motivation. Their constant companionship and care were very heartwarming throughout my journey as a PhD candidate.

TABLE OF CONTENTS

ACKNOWLEDGEMENT	ii
TABLE OF CONTENTS	iii
LIST OF TABLES	x
LIST OF FIGURES	xii
LIST OF SYMBOLS	xvi
LIST OF ABBREVIATIONS	xviii
LIST OF APPENDICES	xxi
ABSTRAK	xxii
ABSTRACT	xxiv
CHAPTER 1 INTRODUCTION	1
1.1 Overview.....	1
1.2 Objectives of this study	5
CHAPTER 2 LITERATURE REVIEW	6
2.1 Plastics	6
2.2 Bio-based polymer from microorganism.....	8
2.3 Polyhydroxyalkanoates (PHAs)	9
2.4 Type of PHAs.....	12
2.4.1 Poly(3-hydroxybutyrate) [P(3HB)].....	12
2.4.2 Poly(3-hydroxybutyrate- <i>co</i> -3-hydroxyhexanoate) [P(3HB- <i>co</i> -3HHx)]	13
2.5 PHA synthases (PhaCs)	14
2.5.1 PhaC from mangrove soil metagenome (PhaC _{BP-M-CPF4})	17
2.6 Metabolic pathway of PHA biosynthesis	18
2.7 3-D structure of PHA synthase (PhaC).....	21
2.8 N-terminal region of PHA synthase (PhaC)	24

2.9	Metabolic engineering of strains for PHA production	26
2.10	Protein engineering of PhaC	28
2.11	Enoyl-CoA hydratase (PhaJ).....	30
2.12	<i>Cupriavidus necator</i> (<i>C. necator</i>)	31
2.13	Granular size and number of PHA granules affecting recovery of PHAs	33
2.14	Molecular weights of PHA	34
2.15	Application of PHA.....	36
CHAPTER 3 METHODOLOGY.....		39
3.1	General techniques	39
3.1.1	Aseptic techniques	39
3.1.2	Sterilization.....	39
3.1.3	Measurement of optical density (OD) and pH.....	39
3.2	Media preparation.....	40
3.2.1	Lysogeny broth (LB).....	40
3.2.2	Nutrient-rich (NR) medium.....	40
3.2.3	Simmons citrate agar.....	41
3.2.4	Mineral salt medium (MM)	41
3.2.5	Super Optimal broth with Catabolite repression (SOC) medium.....	43
3.2.6	Preparation of antibiotic stock solution.....	43
3.3	Carbon sources	43
3.3.1	Crude palm kernel oil (CPKO).....	43
3.3.2	Fructose	44
3.4	Bacterial strains and plasmid	44
3.5	General molecular biology techniques	46
3.5.1	Primer design.....	46
3.5.2	Plasmid extraction.....	47
3.5.3	Preparation of chemically competent cells.....	48

3.5.4	Gel electrophoresis.....	49
3.5.5	Polymerase chain reaction (PCR).....	49
3.5.6	Gel purification.....	53
3.5.7	Digestion of PCR product and plasmid vector by restriction enzyme	54
3.5.8	PCR product purification.....	55
3.5.9	DNA quantification and quality analysis	56
3.5.10	Cloning.....	56
	3.5.10(a) Ligation.....	56
	3.5.10(b) In-fusion cloning.....	57
3.5.11	Transformation of the plasmid into <i>E. coli</i>	58
3.5.12	Colony PCR.....	59
3.5.13	Bacterial transconjugation.....	60
3.5.14	DNA sequencing.....	61
3.5.15	Total mRNA extraction.....	61
3.5.16	Total mRNA quantification and quality analysis	63
3.5.17	Conversion of mRNA to cDNA	64
3.5.18	Quantitative polymerase chain reaction (qPCR)	64
3.5.19	qPCR validation analysis.....	65
	3.5.19(a) Amplification efficiency.....	65
	3.5.19(b) Specificity.....	66
	3.5.19(c) qPCR data analysis.....	66
3.5.20	Bradford Reagent.....	66
3.5.21	20% sodium dodecyl sulfate (SDS) solution.....	67
3.5.22	10% Ammonium persulfate (APS) solution.....	67
3.5.23	Sodium dodecyl sulfate polyacrylamide gel electrophoresis (SDS-PAGE)	67
3.5.24	12.5% Separating gel	69

3.5.25	5% Stacking gel.....	70
3.5.26	Running buffer.....	71
3.5.27	5 × Laemmli buffer.....	72
3.5.28	Coomassie Blue staining solution.....	73
3.5.29	Destaining solution.....	73
3.6	Prediction of PhaC _{BP-M-CPF4} structure.....	74
3.7	Construction of PHB ⁻ 4 harbouring the truncated <i>phaC</i> _{BP-M-CPF4}	74
3.8	Characterization of N-terminal truncated PhaC _{BP-M-CPF4} mutants in <i>C. necator</i> mutant, PHB ⁻ 4.....	77
3.8.1	PHA biosynthesis.....	77
3.8.1(a)	Preculture preparation.....	77
3.8.1(b)	One-stage cultivation.....	77
3.8.1(c)	Bacteria cell harvesting and lyophilization.....	77
3.8.1(d)	Determination of dry cell weight (DCW).....	78
3.8.2	Determination of PHA content and monomer composition.....	78
3.8.2(a)	Methanolysis solution.....	78
3.8.2(b)	Caprylic acid methyl ester (CME).....	79
3.8.2(c)	Sample preparation for gas chromatography (GC) analysis.....	79
3.8.2(d)	Gas chromatography (GC) analysis.....	80
3.8.3	Determination of molecular weights of the PHA produced.....	82
3.8.3(a)	PHA extraction from lyophilized bacteria cell.....	82
3.8.3(b)	Gel permeation chromatography (GPC) analysis.....	83
3.8.4	Determination of granule morphology in PHB ⁻ 4 transformants harbouring full-length PhaC _{BP-M-CPF4} , G8, A27 and T74.....	83
3.8.4(a)	Preparation of sample for transmission electron microscopy (TEM).....	83
3.8.4(b)	Transmission electron microscopy (TEM).....	85
3.8.5	Phase contrast microscopy analysis.....	85

3.8.6	Determination of expression of full-length PhaC _{BP-M-CPF4} and its N-terminal truncated mutants.....	86
3.8.7	Prediction of mRNA secondary structure	86
3.9	Construction of production strain <i>C. necator</i> mutant, Re2058 harbouring PhaC _{BP-M-CPF4} G8.....	87
3.10	Characterization of production strain <i>C. necator</i> , Re2058 harbouring pBG8	89
3.11	Characterization of PHA granules accumulated in production strain <i>C. necator</i> , Re2058 harbouring pBG8.....	89
3.11.1	Partial PHA purification using mealworm	89
3.11.2	Determination of residual protein from fecal pellets	90
3.11.2(a)	Removal of residual proteins from fecal pellets	90
3.11.2(b)	SDS-PAGE analysis.....	90
3.11.2(c)	Determination of protein concentration from the fecal pellets	91
3.11.3	Granule morphology of purified PHA granules from mealworm extraction.....	91
3.12	High cell density production using production strain <i>C. necator</i> , Re2058 harbouring pBG8.....	91
3.12.1	Preparation of 13 L fermenter	91
3.12.2	Preparation of seed culture	92
3.12.3	Fed-batch fermentation using a 13 L fermenter	92
3.13	Statistical analysis	93
CHAPTER 4 RESULTS.....		94
4.1	Predicted structure of PhaC _{BP-M-CPF4}	95
4.2	Construction of <i>C. necator</i> PHB ⁻ 4 harbouring N-terminal region truncated PhaC _{BP-M-CPF4}	97
4.3	Production of P(3HB) and P(3HB-co-3HHx) by <i>C. necator</i> PHB ⁻ 4 harbouring full-length PhaC _{BP-M-CPF4} and its N-terminal truncated mutants	101
4.4	Decreased in expression of N-terminal region truncated <i>phaC</i> _{BP-M-CPF4}	105
4.5	Predicted secondary mRNA structure of full-length PhaC _{BP-M-CPF4}	106

4.6	Decrease in the percentage of PHA granules and increase in diameter of PHA granules as more N-terminal region of PhaC _{BP-M-CPF4} and its N-terminal truncated mutants	108
4.7	Decrease in the number of PHA accumulating bacteria cells.....	111
4.8	Construction of production strain <i>C. necator</i> Re2058 harbouring N-terminal truncated PhaC _{BP-M-CPF4} G8.....	112
4.9	Production of P(3HB) and P(3HB-co-3HHx) by <i>C. necator</i> Re2058 harbouring pBG8 compared to <i>C. necator</i> Re2058 harbouring pHTI-C _{BP-M-CPF4}	115
4.10	Altered granule morphology of N-terminal truncated PhaC _{BP-M-CPF4} G8 compared to its full-length.....	117
4.11	Comparison of residual protein of fecal pellets after mealworm extraction.	118
	4.11.1 SDS-PAGE analysis.....	118
	4.11.2 Bradford assay analysis.....	119
4.12	Increased in the size of the purified PHA granules extracted using mealworms	120
4.13	High-cell density production using <i>C. necator</i> Re2058 harbouring N-terminal truncated PhaC _{BP-M-CPF4} G8	123
CHAPTER 5 DISCUSSIONS.....		125
5.1	Cloning and expression of full-length PhaC _{BP-M-CPF4} and its N-terminal mutants in <i>C. necator</i> PHB ⁻ 4.....	125
5.2	PHA biosynthesis of <i>C. necator</i> PHB ⁻ 4 harbouring full-length PhaC _{BP-M-CPF4} and its N-terminal truncated mutants using fructose and CPKO	127
5.3	N-terminal truncation of PhaCs affected the <i>M_w</i> of PHA produced.....	130
5.4	N-terminal truncation of PhaC _{BP-M-CPF4} affects its granular morphology	135
5.5	N-terminal truncation improved PhaC _{BP-M-CPF4}	138
5.6	Construction of an efficient production of P(3HB-co-3HHx)	139
5.7	PHA biosynthesis of <i>C. necator</i> Re2058 transformants using fructose and CPKO.....	139
5.8	PHA granules from N-terminal truncated PhaC _{BP-M-CPF4} for better PHA recovery	141
5.9	High-cell density P(3HB-co-3HHx) production using <i>C. necator</i> Re2058 harbouring pBG8.....	145

CHAPTER 6	CONCLUSION	147
CHAPTER 7	RECOMMENDATIONS FOR FUTURE WORK.....	150
REFERENCES	152
APPENDICES		
LIST OF PUBLICATIONS		

LIST OF TABLES

		Page
Table 2.1	Examples of bio-based polymer.....	9
Table 2.2	Different classes of PhaCs based on their subunit compositions and substrate specificities.	16
Table 3.1	Components of MM.....	42
Table 3.2	Components of trace elements.....	42
Table 3.3	List of strains and plasmids used in this study.	44
Table 3.4	Schematic illustration of genotypes of <i>C. necator</i> H16 wild type, <i>C. necator</i> mutant host PHB ⁻ 4 and Re2058 harbouring plasmid pBBR1MCS2 with <i>phaC</i> _{BP-M-CPF4} and its truncated mutants and pBG8 harboring truncated <i>phaC</i> _{BP-M-CPF4} G8 respectively. Deleted genes are indicated using dash lines.	46
Table 3.5	List of primers used in this study.....	51
Table 3.6	PCR reaction mixture for amplification of truncated <i>phaC</i> _{BP-M-CPF4}	52
Table 3.7	Thermocycling condition for amplification of truncated <i>phaC</i> _{BP-M-CPF4}	52
Table 3.8	Pairing of primers, DNA template, and PCR product.	53
Table 3.9	Reaction mixture for plasmid vector and PCR product restriction. ..	55
Table 3.10	Ligation reaction mixture.....	57
Table 3.11	In-Fusion cloning reaction mixture.	58
Table 3.12	PCR reaction mixture for colony PCR.....	59
Table 3.13	Thermocycling condition for colony PCR.	60
Table 3.14	Components of enzymatic lysis buffer.	63
Table 3.15	qPCR reaction mix.....	65

Table 3.16	Thermocycling condition for qPCR reaction.	65
Table 3.17	Components of 3 M Tris-Cl solution.	69
Table 3.18	Components of 1:1 gel buffer solution.	70
Table 3.19	Components of 12.5% separating gel solution.	70
Table 3.20	Components of 0.5 M Tris-Cl, 0.22 M NaH ₂ PO ₄ solution.	71
Table 3.21	Components of stacking solution.	71
Table 3.22	Components of 5% stacking gel solution.	71
Table 3.23	Components of 7 × running buffer.	72
Table 3.24	Components of 1 × running buffer.	72
Table 3.25	Components of 10 × Laemmli buffer.	72
Table 3.26	Components of 5 × Laemmli buffer.	73
Table 3.27	Components of Coomassie Blue staining solution.	73
Table 3.28	Components of destaining solution.	74
Table 3.29	Feeding strategy of CPKO and urea throughout the fermentation run.	93
Table 4.1	PHA production of <i>C. necator</i> PHB ⁻ 4 harbouring full-length PhaC _{BP-M-CPF4} with its N-terminal truncated PhaC _{BP-M-CPF4} mutants.	103
Table 4.2	PHA production of <i>C. necator</i> Re2058 harbouring pHTI- <i>C</i> _{BP-M-CPF4} and <i>C. necator</i> Re2058 harbouring pBG8.	116
Table 4.3	Molar composition of P(3HB- <i>co</i> -8 mol% 3HHx) produced by <i>C. necator</i> Re2058 harbouring pHTI- <i>C</i> _{BP-M-CPF4} compared to <i>C. necator</i> Re2058 harbouring pBG8 with their respective <i>M</i> _w	124

LIST OF FIGURES

		Page
Figure 2.1	PHA accumulated in bacteria cells. (A) Phase contrast light microscopy image of PHA granules (white) in mutant <i>C. necator</i> Re2058 harbouring pHTI- <i>C</i> _{BP-M-CPF4} plasmid cultured in 50 mL minimal medium supplemented with 50 µg/mL kanamycin, 1% (w/v) crude palm kernel oil as a carbon source and 0.054% (w/v) urea as a nitrogen source, shaken at 200 rpm for 48 h in 30 °C. Magnification: 1000×. The PHA accumulated was P(3HB- <i>co</i> -9 mol% 3HHx) and the PHA content was at 76 wt % of the dry cell weight. (B) Schematic diagram of PHA granule (white) surrounded by proteins. PHA can be surrounded by PHA synthase (PhaC) (black), depolymerase (blue), PHA-granules associated protein (PGAP) (red), and phasin (green).....	10
Figure 2.2	Chemical structure of P(3HB). “n” represents the number of repeated units.....	13
Figure 2.3	Chemical structure of P(3HB- <i>co</i> -3HHx). “X” and “Y” represent the number of repeated units.	14
Figure 2.4	Metabolic pathway of PHA biosynthesis. The black box, red box, blue box, green box, and purple box represent the pathway used by bacteria for the production of P(3HB), P(3HB- <i>co</i> -3HHx) using oil, P(3HB- <i>co</i> -3HHx) using sugar, P(3HB- <i>co</i> -3HV), and P(3HB- <i>co</i> -4HB) respectively.	21
Figure 3.1	Overall schematic diagram for construction of <i>C. necator</i> mutant, PHB ⁻ 4 harbouring pBBR1- <i>C</i> _{BP-M-CPF4} G8, A27, T74, and D104.	76
Figure 3.2	Overall schematic diagram for construction of production strain <i>C. necator</i> mutant, Re2058 harbouring pBG8.	88
Figure 4.1	Predicted N-terminal structure of PhaC _{BP-M-CPF4} . (A) Predicted N-terminal tertiary structure of PhaC _{BP-M-CPF4} using AlphaFold2 program. The colours indicate in the predicted structure represent	

the level of confidence in the prediction. The black circle indicates the structure of the N-terminal which was predicted to have low confidence. The lines indicate the truncation point of the N-terminal. (B) Predicted secondary structure of N-terminal from PhaC_{BP-M-CPF4} using the PSIPRED server. The arrow shows the truncation point of A27. (C) Predicted secondary structure of the N-terminal region using a combination of AlphaFold2 program and PSIPRED server. The truncation points are indicated with black lines..... 97

Figure 4.2 Gel electrophoresis gel image. (A) Gel electrophoresis image of extracted pBBR1-C_{BP-M-CPF4} from PHB⁻4/pBBR1-C_{BP-M-CPF4}. (B) Gel electrophoresis image of gel extracted PCR products of *phaC*_{BP-M-CPF4} G8, A27, T74, and D104. (C) Gel electrophoresis image of *Hind*III and *Apa*I digested pBBR1-ProC_n. (D) Gel electrophoresis image of *Hind*III and *Apa*I digested *phaC*_{BP-M-CPF4} G8, A27, T74, and D104..... 99

Figure 4.3 Gel electrophoresis image. (A) Gel electrophoresis image of colony PCR *E. cloni*® 10G harbouring *phaC*_{BP-M-CPF4} G8, A27, T74, and D104. (B) Gel electrophoresis image of pBBR1-C_{BP-M-CPF4} G8, A27, T74, and D104. (C) Gel electrophoresis image of colony PCR *E. coli* S17-1 harbouring *phaC*_{BP-M-CPF4} G8, A27, T74, and D104. (D) Gel electrophoresis image of colony PCR *C. necator* PHB⁻4 harbouring *phaC*_{BP-M-CPF4} G8, A27, T74, and D104..... 100

Figure 4.4 Gene expression of full-length *phaC*_{BP-M-CPF4} compared to its N-terminal truncated mutants. 106

Figure 4.5 Predicted secondary structure of transcribed mRNA for full-length *phaC*_{BP-M-CPF4}. The predicted secondary structure of transcribed mRNA starts from the predicted transcription start site. The start codon was indicated using a blue square. The cyan and blue oval indicated stem-loop structures formed by nucleotides that encoded for the first seven amino acids while the red oval indicated the

stem-loop structures formed by the nucleotide encoded for the first 26 amino acid residues. Points of truncation for G8, A27, T74, and D104 were indicated using green, orange, brown, and purple arrows respectively. 108

Figure 4.6 Granule morphology of P(3HB) granules in *C. necator* PHB⁻4 harbouring the full-length PhaC_{BP-M-CPF4} and its N-terminal truncated mutants which was examined using TEM. Pie charts illustrating the percentage of bacteria cells with their number of PHA granules were plotted. The mean diameter of the PHA granules accumulated by transformants harbouring full-length PhaC_{BP-M-CPF4} and its N-terminal truncated mutants are shown in the upper-right corner of the TEM images. The oozing phenomenon is highlighted with black circles. The TEM images shown reflect the corresponding number of granules in each bacteria cell harbouring (A) full-length PhaC_{BP-M-CPF4}, Magnification: 4000 ×, (B) G8, Magnification: 3200 ×, (C) A27, Magnification: 4000 ×, and (D) T74, Magnification: 4000 ×. 111

Figure 4.7 Phase contrast microscopy images of *C. necator* PHB⁻4 harbouring the (A) full-length PhaC_{BP-M-CPF4} (B) G8, (C) A27, and (D) T74. Magnification: 1000 ×. 112

Figure 4.8 Gel image of electrophoresis of (A) RBS_G8, (B) linearized pCB113, (C) colony PCR for *E. cloni*® 10G (Lucigen, USA) harbouring pBG8, (D) extracted pBG8 plasmid from *E. cloni*® 10G, (E) colony PCR for *E. coli* S17-1 harbouring pBG8, (F) colony PCR of *C. necator* Re2058 harbouring pBG8. 114

Figure 4.9 Granule morphology of P(3HB) granules in (A) *C. necator* Re2058 harbouring the full-length PhaC_{BP-M-CPF4}, Magnification: 2200 × and (B) *C. necator* Re2058 harbouring N-terminal truncated PhaC_{BP-M-CPF4} G8, Magnification: 2500 × which was examined using TEM. Pie charts illustrating the percentage of bacteria with its number of PHA granules were plotted. The TEM images shown reflect the corresponding number of granules in each bacterial cell.

	The granule mean diameters were shown on the upper-right of the TEM images.	118
Figure 4.10	SDS gel image of the denatured residual proteins from the PHA granules of <i>C. necator</i> H16 wild type (Lane 1), <i>C. necator</i> Re2058 harbouring pHTI- <i>C</i> _{BP-M-CPF4} (Lane 2) and <i>C. necator</i> Re2058 harbouring pBG8 (Lane 3) extracted using mealworm. M: Protein ladder. The protein bands were indicated in the red box.	119
Figure 4.11	Amount of protein denatured from the washed fecal pellet from <i>C. necator</i> H16 wild type, <i>C. necator</i> Re2058 harbouring pHTI- <i>C</i> _{BP-M-CPF4} , and <i>C. necator</i> Re2058 harbouring pBG8. The protein concentrations were obtained using Bradford assay where the absorbances were taken at OD _{595nm}	120
Figure 4.12	SEM images of purified PHA granule recovered from (A) <i>C. necator</i> H16 wild type, (B) <i>C. necator</i> Re2058/pHTI- <i>C</i> _{BP-M-CPF4} , and (C) <i>C. necator</i> Re2058/pBG8. Magnification: 3000 ×. Scale bar: 1 μm.	122
Figure 4.13	7 L fed-batch fermentation run of <i>C. necator</i> Re2058/pBG8. PHA content, dry cell weight, wet cell weight, 3HB, and 3HHx molar composition change throughout the fermentation run.	124

LIST OF SYMBOLS

α	Alpha
~	Approximately
β	Beta
Da	Dalton
°C	Degree Celsius
Δ	Delta
wt%	Dry weight percent
γ	Gamma
g	Gram
h	Hour
∞	Infinity
kDa	Kilodalton
kPa	Kilopascal
L	Liter
μg	Microgram
μL	Microliter
μM	Micromolar
mg	Milligram
mL	Milliliter
mM	Millimolar
min	Minute
mol%	Mole percent
ng	Nanogram
nm	Nanometer

nM	Nanomolar
%	Percentage
±	Plus-minus
psi	Pounds per square inch
(R)	Rectus isomer
rpm	Revolutions per minute
s	Second
(S)	Sinister isomer
×	Times
× <i>g</i>	Times gravity
V	Volt
v/v	Volume per volume
w/v	Weight per volume

LIST OF ABBREVIATIONS

3H4MV	3-hydroxy-4-methylvalerate
3HB	3-hydroxybutyrate
3HB-CoA	3-hydroxybutyryl-CoA
3HHp	3-hydroxyheptanoate
3HHx	3-hydroxyhexanoate
3HHx-CoA	3-hydroxyhexanoyl-CoA
3HV	3-hydroxyvalerate
4HB	4-hydroxybutyrate
4HB-CoA	4-hydroxybutyryl-CoA
5HV	5-hydroxyvalerate
ANOVA	One-way analysis of variance
β -ME	β -mercaptoethanol
C	Cysteine
CME	Caprylic methyl ester
CoA	coenzyme A
cDNA	Complementary deoxyribonucleic acid
CPKO	Crude palm kernel oil
C-terminus	Carboxy-terminus
Ct	Cycle threshold
D	Aspartic acid
DNA	Deoxyribonucleic acid
dNTP	Deoxyribonucleoside triphosphate
DCW	Dry cell weight
DTT	Dithiothreitol
EDTA	Ethylenediaminetetraacetic acid
GC	Gas chromatography
gDNA	Genomic DNA
GPC	Gel permeation chromatography
H	Histidine
HA	Hydroxyacyl
HA-CoA	Hydroxyacyl-CoA

HPLC	High-performance liquid chromatography
LB	lysogeny broth
LDPE	Low-density polyethylene
mRNA	Messenger RNA
MM	Mineral medium
M_n	Number-average molecular weight
M_w	Weight-average molecular weight
NR	Nutrient-rich
N-terminus	Nitrogen terminus
OsO ₄	Osmium tetroxide
PDI	Polydispersity index
pLDDT	Per-residue estimate of its confidence
PHA	Polyhydroxyalkanoate
P(3HB)	Poly(3-hydroxybutyrate)
P(3HB- <i>co</i> -3HHx)	Poly[(<i>R</i>)-3-hydroxybutyrate- <i>co</i> -(<i>R</i>)-3-hydroxyhexanoate]
PhaA	Beta-ketothiolase
PhaB	NADPH-dependent acetoacetyl-CoA reductase
PhaC _{BP-M-CPF4}	PhaC isolated from mangrove soil metagenome
PhaC _{Cs}	PhaC from <i>Chromobacterium</i> sp. USM2
PhaC _{Ra}	PhaC from <i>Rhodococcus aetherivorans</i> I24
PhaC _{Ah}	PhaC from <i>Aeromonas hydrophila</i> 4AK4
PhaC _{Ac}	PhaC from <i>Aeromonas caviae</i>
PhaC _{Cn}	PhaCs from <i>Cupriavidus necator</i> H16
PhaC _{Pa}	PhaC from <i>Pseudomonas aeruginosa</i>
PhaE	PHA synthase subunit E
PhaG	3-hydroxyacyl-ACP-CoA transferase
PhaJ	(<i>R</i>)-specific enoyl-CoA hydratase
PhaP	Phasin
PhaR	PHA synthase subunit R
PhaZ	PHA depolymerase
PO	Palm olein
PP	Polypropylene
ProC	Pyrroline-5-carboxylate reductase
PS	Polystyrene

PSI-BLAST	Position-Specific Iterative Basic Local Alignment Search Tool
PSIPRED	PSI-blast based secondary structure prediction
P-value	Probability value
PVC	Polyvinyl chloride
qPCR	Quantitative polymerase chain reaction
RNA	Ribonucleic acid
RBS	Ribosomal binding sites
SCL	Short-chain-length
SD	Standard deviation
SDS	Sodium dodecyl sulfate
SDS-PAGE	Sodium dodecyl sulfate polyacrylamide gel electrophoresis
SOB	Super Optimal Broth
TAE	Tris-acetate-EDTA
TCA	Tricarboxylic acid
TEM	Transmission electron microscopy
T_g	Glass transition temperature
T_m	Melting temperature
UHMW	Ultrahigh-molecular-weight
UV	Ultraviolet

LIST OF APPENDICES

- Appendix A Approval by the Institutional Biosafety Committee
- Appendix B Total mRNA quantity and quality analysis
- Appendix C qPCR validation analysis

**PEMANGKASAN N-TERMINAL PADA SINTASE PHA
(PhaC_{BP-M-CPF4}) SEBAGAI STRATEGI UNTUK MEMPERBAIK CIRI
POLIHIDROKSIALKANOAT OLEH Cupriavidus necator**

ABSTRAK

Polihidroksialkanoat (PHA) adalah sejenis poliester berasaskan bio dan boleh terbiodegradasi, yang disintesis oleh kebanyakan bakteria dan arkea dalam keadaan lebihan karbon dan kekurangan nutrien. Antara jenis PHA, poli[(R)-3-hidroksibutirat-ko-(R)-3-hidroksiheksanoat] [P(3HB-co-3HHx)] dilaporkan mempunyai persamaan yang hampir dengan polipropilena (PP) dan polietilena ketumpatan rendah (LDPE) komersial. PHA sintase (PhaC) adalah enzim yang paling penting dalam biosintesis PHA kerana ia menentukan sifat PHA yang dihasilkan. Struktur PhaC terdiri daripada terminal N dan C-terminal. Sehingga kini, tidak banyak PhaC yang produktif dilaporkan untuk penghasilan P(3HB-co-3HHx). Kajian terdahulu menunjukkan bahawa PhaC yang diasingkan daripada metagenom paya bakau, PhaC_{BP-M-CPF4}, adalah PhaC yang cekap untuk penghasilan P(3HB-co-3HHx). N-terminal mempengaruhi keperincian substrat dan dimerisasi untuk fungsi PhaC, morfologi granul, dan berat molekul PHA yang dihasilkan. Dalam kajian ini, struktur penuh atau hampir penuh PhaC_{BP-M-CPF4} berjaya diramal menggunakan perisian AlphaFold dan PSIPRED server. N-terminal PhaC_{BP-M-CPF4} telah dipangkas berdasarkan strukturnya yang diramal, menghasilkan 4 mutan, iaitu PhaC_{BP-M-CPF4} G8, A27, T74, dan D104, yang kemudian diklon ke dalam *Cupriavidus necator* PHB⁻4. Antara mutan-mutan yang diklon, PhaC_{BP-M-CPF4} G8 menunjukkan peningkatan sifat PHA seperti berat molekul purata berat (M_w) yang lebih tinggi, dan kebanyakan granul PHA yang lebih besar dan tunggal berbanding PhaC_{BP-M-CPF4}

panjang penuh tanpa menjejaskan kandungan PHA dan berat sel kering. $\text{PhaC}_{\text{BP-M-CPF4}}$ G8 kemudian diklon dan ditranskonjugasi ke dalam strain *C. necator* Re2058, menghasilkan *C. necator* Re2058 yang mengandung pBG8. *C. necator* Re2058 yang baharu dengan pBG8 juga mengumpul M_w yang lebih tinggi dan lebih banyak granul PHA yang lebih besar dan tunggal berbanding *C. necator* Re2058 dengan pHTI- $\text{C}_{\text{BP-M-CPF4}}$. Palet najis yang dicuci air daripada *C. necator* Re2058 dengan pBG8 mempunyai kepekatan protein yang lebih rendah berbanding *C. necator* H16 jenis liar dan Re2058 dengan pHTI- $\text{C}_{\text{BP-M-CPF4}}$. Akhir sekali, *C. necator* Re2058 dengan pBG8 dinilai keupayaannya untuk pengeluaran sel berketumpatan tinggi menggunakan penapaian berskala 13 L dan berjaya mengumpul P(3HB-co-8 mol% 3HHx) dengan kandungan PHA setinggi 66.6% dan M_w setinggi 1.6×10^6 Da, yang lebih tinggi berbanding P(3HB-co-8 mol% 3HHx) yang dihasilkan oleh *C. necator* Re2058 dengan pHTI- $\text{C}_{\text{BP-M-CPF4}}$.

**N-TERMINAL TRUNCATION OF PHA SYNTHASE (PhaC_{BP-M-CPF4})
AS A STRATEGY FOR IMPROVED POLYHYDROXYALKANOATE
PROPERTIES BY Cupriavidus necator**

ABSTRACT

Polyhydroxyalkanoate (PHA) is a type of bio-based and biodegradable polyester, synthesized by most bacteria and archaea under excess carbon and limited nutrient conditions. Among the types of PHA, poly[(*R*)-3-hydroxybutyrate-*co*-(*R*)-3-hydroxyhexanoate] [P(3HB-*co*-3HHx)] is reported to have a close resemblance to the commercial polypropylene (PP) and low-density polyethylene (LDPE). PHA synthase (PhaC) is the most important enzyme in PHA biosynthesis as it determines the properties of the PHA produced. The structure of a PhaC consists of an N- and C-terminal. To date, there are not many productive PhaCs reported for the production of P(3HB-*co*-3HHx). Previous studies have shown that PhaC isolated from mangrove soil metagenome, PhaC_{BP-M-CPF4} is an efficient PhaC for P(3HB-*co*-3HHx) production and N-terminal influences substrate specificity and dimerization for the PhaC to function, granule morphology and molecular weight of PHA produced. The full-length or nearly full-length structure of PhaC_{BP-M-CPF4} was successfully predicted using the AlphaFold software and PSIPRED server. The N-terminal of PhaC_{BP-M-CPF4} was truncated based on its predicted structure giving rise to 4 N-terminal truncated mutants, PhaC_{BP-M-CPF4} G8, A27, T74, and D104 and cloned into *Cupriavidus necator* PHB⁻4. Among the N-terminal truncated mutants, PhaC_{BP-M-CPF4} G8 demonstrated improved properties of PHA such as higher weight-average molecular weight (M_w), and in mostly single larger PHA granules compared to that of full-length PhaC_{BP-M-CPF4} without compromising the PHA content

and dry cell weight. The PhaC_{BP-M-CPF4} G8 was then cloned and transconjugated into a production strain *C. necator* Re2058 giving rise to *C. necator* Re2058 harbouring pBG8. The new *C. necator* Re2058 harbouring pBG8 also accumulated higher M_w and more single larger PHA granules compared to that of *C. necator* Re2058 harbouring pHTI-*C*_{BP-M-CPF4}. The water-washed fecal pellet of *C. necator* Re2058 harbouring pBG8 had lower protein concentration compared to that of *C. necator* H16 wild type and Re2058 harbouring pHTI-*C*_{BP-M-CPF4}. Lastly, *C. necator* Re2058 harbouring pBG8 was evaluated for its ability for high-cell-density production using a 13 L fermenter and managed to accumulate P(3HB-*co*-8 mol% 3HHx) with PHA content as high as 66.6% and M_w as high as 1.6×10^6 Da which was higher compared to P(3HB-*co*-8 mol% 3HHx) produced by *C. necator* Re2058 harbouring pHTI-*C*_{BP-M-CPF4}.

CHAPTER 1

INTRODUCTION

1.1 Overview

Plastic is undoubtedly the most used material compared to other materials like wood, metal, and the like in various applications because it is lightweight, corrosion-resistant, resilient, and easy to process (Shrivastava, 2018). On the flip side, these commercial plastics are non-biodegradable and hence, cause serious environmental pollution upon disposal, particularly single-use plastics. The gradual worsening of plastic pollution has encouraged the development of biodegradable plastics. Among the most promising types of biodegradable plastics is polyhydroxyalkanoates (PHAs), which is a type of polyester accumulated by most bacteria and archaea from renewable sources under the condition where there are excess in carbon sources and limited nutrients (Stubbe & Tian, 2003). PHAs are potential biomaterials to replace commercial plastics in certain applications such as single-use plastics as they both have similar properties but PHAs can be degraded through microbial metabolism (Passos *et al.*, 2015).

To date, there are over 150 different types of PHA monomers identified, and it is believed that more new PHA monomers are to be identified in the near future (Steinbüchel & Valentin, 1995). PHA polymers consisting of only one PHA monomer are known as homopolymers. PHA polymers consisting of two different PHA monomers are known as copolymers while those consisting of three are known as terpolymers. PHAs consisting of different PHA monomers may differ in properties. For instance, poly(3-hydroxybutyrate) [P(3HB)] comprising of 4-carbon 3-hydroxybutyrate as the smallest building block, is stiff, brittle, has very high crystallinity and melting point higher than 170 °C, making them hard to process and

limit their application (Sudesh *et al.*, 2000). To improve such properties, other PHA monomers like 4-hydroxybutyrate (4HB), 3-hydroxyvalerate (3HV), 5-hydroxyvalerate (5HV), and 3-hydroxyhexanoate (3HHx) are often incorporated into the homopolymer of P(3HB) making it more flexible, a lower melting point, lower Young's modulus, higher elongation to break and practical industrial-desired materials (Bhubalan *et al.*, 2010; Doi *et al.*, 1995; Lakshmanan *et al.*, 2019).

The most important catalysts in PHA biosynthesis is the PHA synthase (PhaC) enzyme, which is encoded by the *phaC* gene because it determines the types of monomers incorporated into the PHA polymer and hence, determines the properties of the PHA produced. Long chains of PHA are synthesized through polymerization of the monomeric acyl-moieties of the acyl-coenzyme A substrate by PhaC. To date, there are only two crystal structures of PhaCs reported by three independent research groups. They are the crystal structure of PhaC from *Cupriavidus necator* H16 (PhaC_{Cn}) and PhaC from *Chromobacterium* sp. USM2 (PhaC_{Cs}) (Chek *et al.*, 2017; Kim *et al.*, 2017a; Wittenborn *et al.*, 2016). However, all the reported structures lacked structural information about the N-terminal domain and, had limited knowledge of the N-terminal's involvement in the polymerization of hydrophilic monomers into chains of hydrophobic polymers. In general, the structure of a PhaC consists of two parts: the N-terminal and the C-terminal domain. Previous studies showed that the N-terminal region can alter the substrate specificity, and dimerization of PhaC, granule morphology, and the molecular weights of the PHA synthesized (Lim *et al.*, 2021).

P(3HB-*co*-3HHx) is one of the industrially desired PHA due to its similar resemblance to polypropylene (PP) and low-density polyethylene (LDPE) (Doi, 1990). However, there are just a few reported efficient strains for P(3HB-*co*-3HHx) production (Budde *et al.*, 2011; Tan *et al.*, 2020). Hence, there is a need for an efficient

strain for P(3HB-*co*-3HHx) production. To construct an efficient strain, an efficient PhaC must first be obtained. Even so, there is only a handful of good PhaCs for P(3HB-*co*-3HHx) production such as PhaC from *Aeromonas caviae* (PhaC_{Ac}), PhaC from *Rhodococcus aetherivorans* I24 (PhaC_{2Ra}), PhaC from *Aeromonas hydrophila* 4AK4 (PhaC_{Ah}), and PhaC that is locally isolated from mangrove soil metagenome in Balik Pulau, Penang (PhaC_{BP-M-CPF4}) (Budde *et al.*, 2011; Foong *et al.*, 2018; Fukui & Doi, 1997; Yu *et al.*, 2020). A good PhaC for PHA production is a PhaC that can accumulate a high amount of PHA with desirable molar compositions and molecular weights in single large PHA granules. Among the PhaCs reported, PhaC_{BP-M-CPF4} has caught the attention of researchers due to its ability to incorporate up to six different types of short- and medium-chain length monomers like 3-hydroxybutyrate (3HB), 3-hydroxyvalerate (3HV), 4-hydroxybutyrate (4HB), 3-hydroxy-4-methylvalerate (3H4MV), 5-hydroxyvalerate (5HV) and 3-hydroxyhexanoate (3HHx) in the presence of suitable precursor substrates (Foong *et al.*, 2018).

To date, only a limited number of productive strains have been developed for the production of P(3HB-*co*-3HHx) copolymer, including *C. necator* Re2058/pCB113, *C. necator* Re2058/pHTI-C_{BP-M-CPF4}, *Halomonas bluephagenesis* G34, and *C. necator* NSDG-GG-HC/pBPP-C_{Cr_{Me}J_{Ac}-emd_{Mm} (Budde *et al.*, 2011; Tan *et al.*, 2020; Wang *et al.*, 2023; Zhang *et al.*, 2019). This highlights the pressing need to develop additional production strains for P(3HB-*co*-3HHx) synthesis. Several criteria must be met to successfully develop a production strain for P(3HB-*co*-3HHx) copolymer synthesis. The first is high PHA content, as more PHA can be accumulated by the strain which will directly increase the production of PHA. Next is suitable properties of PHA accumulated with its applications. Different 3HHx monomer compositions can lead to various properties of the PHA produced. The higher the}

3HHx monomer composition of P(3HB-*co*-3HHx), the more flexible the PHA will be. Too low 3HHx monomer composition will lead to too brittle P(3HB-*co*-3HHx) while too high 3HHx monomer composition will lead to weak and too flexible P(3HB-*co*-3HHx). Besides 3HHx monomer composition, molecular weights of the P(3HB-*co*-3HHx) must also be considered as low molecular weights will lead to weaker mechanical strength of P(3HB-*co*-3HHx) accumulated. Last but not least are the downstream processes of PHA recovery and purification. While a strain may accumulate a high PHA content, inefficient recovery can result in reduced yields, ultimately lowering the amount of PHA obtained from production.

In this study, the N-terminal of the PhaC_{BP-M-CPF4} was truncated according to its predicted N-terminal secondary structure and evaluated based on the amount of PHA accumulated, molar composition, molecular weights of the PHA accumulated and the granule morphology of PHA granules accumulated in the *C. necator* transformants to screen for an improved PhaC_{BP-M-CPF4}. The relationship between the gene expression of *phaC*_{BP-M-CPF4} with the weight-average molecular weight (M_w) of the P(3HB-*co*-3HHx) produced was also examined using quantitative PCR (qPCR) and gas permeation chromatography (GPC) analysis. The improved N-terminal truncated PhaC_{BP-M-CPF4} mutant was then cloned into a production strain, *C. necator* Re2058, and again evaluated based on its PHA accumulation, molar compositions, M_w of the PHA accumulated, the PHA granule morphology, protein concentration of the washed fecal pellets which contained the PHA granules and size of PHA granules recovered. Last but not least, the ability of the constructed strain for high-cell density production.

1.2 Objectives of this study

- a) To construct an efficient strain for the production of P(3HB-*co*-5 – 8 mol% 3HHx)
- b) To improve the molecular weights of P(3HB-*co*-5 – 8 mol% 3HHx) produced to more than 1×10^6 Da
- c) To improve the purity of the PHA recovered

CHAPTER 2

LITERATURE REVIEW

2.1 Plastics

Plastic is a type of polymer with desirable properties like chemical and UV-resistance, cheap, durability, high thermostability, and good electric insulation. The large varieties of polymers and the versatility of their properties increase their demand for plastic. Consequently, the increase in demand for plastic has increased the production of plastic products. Based on Statista, in 2021, it was projected that the world would produce 390.7 million metric tonnes of plastic, a growth of 4% annually. Since the 1950s, the production of plastic has escalated tremendously. China alone accounts for six to twelve million tonnes of plastic manufactured each month, making Asia the region with the highest output of plastic globally (Statista Research Department, 2022). More than 350 million metric tonnes of plastic waste are produced yearly, and that number is estimated to peak at one billion metric tonnes by 2060. The reduction in plastic waste is only projected to be less than 700 million metric tonnes per year, even with new measures and legislation. Only 15% of plastic waste has been collected for recycling globally, and less than 10% of that gets recycled each year (Tiseo, 2023).

Plastics have indeed become extremely important and indispensable in various fields. Unfortunately, plastic is non-biodegradable which has become one of our biggest concerns. Their non-biodegradability has given rise to plastic pollution and has caused other major impacts to the environment like marine pollution, greenhouse gas production as well as risking human health (Rodrigues *et al.*, 2019; Shen *et al.*, 2020). Plastic waste that has been improperly managed is primarily dumped illegally or burned in open pits, but a substantial quantity also escapes into the environment, including rivers and oceans. Over 100 million tonnes of plastic have accumulated in rivers and

lakes, compared to an estimated 30 million tonnes in the ocean. Such significant plastic waste in waterways can have catastrophic effects on ecosystems and marine life. An estimated more than 80% of the plastic waste dumped into the ocean worldwide comes from Asia while wealthy countries only contribute to about 5% of the ocean's plastic waste. This is because they frequently export to developing countries for processing. However, many of these developing countries lack the capability to handle this enormous amount of plastic waste (Tiseo, 2023).

The further increase in disposable consumer plastic products with ultra-durable properties has further highlighted the fact that plastics are unsustainable (Halden, 2010). Based on a report by Grand View Research, about 33% of the production of plastic in 2022 goes to the packaging industry, with the highest use of plastic compared to other industries. The construction industry came in second with about 20% followed by the consumer goods sector with about 15% to 18% (*Plastic Market Size, Share, Trends & Growth Report, 2030*, n.d.). Besides the packaging industry, the usage of disposable plastic products is also quite worrisome as the usage of these products is very short, for example, plastic bags, disposable cups, and plastic utensils. These products are also known to persist in the environment for quite a long time, hence, giving rise to plastics-exposed biotas. Plastics can also be broken down into debris that can be ingested by small marine animals (Laist, 1997). So far there are more than 260 species of fish, seagulls, invertebrates, turtles, condors, and mammals that have been documented to ingest or entangled by plastic debris. To avoid such problems, one alternative is incineration. Unfortunately, this method is known to generate chemicals and cause severe health issues since the gases emitted can be carcinogenic polychlorinated dibenzo-*p*-dioxins/furans (PCDD/Fs) or organohalogenes (Takasuga *et al.*, 2007).

2.2 Bio-based polymer from microorganism

Bio-based polymers are polymers that have similar properties as the existing petrochemical-based plastics but are made from biological renewable resources and can be polymerized by chemical or biological methods (Harmsen *et al.*, 2014). Hence, they are one of the best alternative materials to replace petrochemical-based plastics such as polyethylene (PE), polyethylene terephthalate (PET), polyamide (PA) polystyrene (PS), polyvinyl chloride (PVC), PP, and LDPE.

These bio-based plastics can be categorized into three distinct categories which are modified natural polymers, biosynthetic polymers, and bio-chemosynthetic polymers (Sudesh & Iwata, 2008). Examples of bio-based polymers are shown in Table 2.1. Modified natural polymers are made from biomass like cellulose and starch. The natural polymers are first obtained and processed through chemical modification forming modified natural polymers (Lu *et al.*, 2005). On the other hand, biosynthetic polymers are polymers that can be synthesized through biological processes. The production of these biosynthetic polymers is often done using bacterial cells (Sudesh *et al.*, 2000). A well-known biosynthetic polymer is PHA which can be accumulated by most bacteria and archaea under the presence of excess carbon but limited nutrients. For bio-chemosynthetic polymers, the monomers are first synthesized biologically using bacterial cells and then polymerized chemically (Jem *et al.*, 2010). A good example is poly(lactic acid), (PLA) which has its monomer first produced by bacteria that is lactic acid through fermentation. The lactic acid is then chemically polymerized into PLA through a chemical method.

Table 2.1: Examples of bio-based polymer.

Category	Processes	Example
Modified natural polymer	Chemical-modified natural polymer	Starch
Biosynthetic polymer	Biosynthesis and modified by metabolic pathways	Cellulose
Bio-chemosynthetic polymer	Biosynthesis of monomers by bacteria's metabolic pathways and polymerized chemical method	P(3HB)

2.3 Polyhydroxyalkanoates (PHAs)

PHA was first discovered by Maurice Lemoigne in *Bacillus megaterium* in the year 1926 (Lemoigne, 1926). The first PHA discovered was P(3HB) homopolymer. PHAs are made up of biopolymeric chains which are made up of hydroxyalkanoates (HA) monomers that are accumulated within the bacterial cells as intracellular carbon storage compounds (Anderson & Dawes, 1990). The number of different genera of both Gram-positive and Gram-negative PHA-producing bacteria has been documented and has increased to more than 75 different genera. It is also believed that more genera are yet to be discovered in the near future (Reddy *et al.*, 2003). To date, there are more than 150 different monomeric blocks of PHA identified (Steinbüchel & Valentin, 1995). PHA are commonly accumulated by most bacteria and archaea under the condition where there is an excess supply of carbon sources accompanied by a limited amount of other nutrients like nitrogen, phosphorus, sulfur, magnesium, and oxygen (Stubbe & Tian, 2003). The PHAs biosynthesized are stored as carbon or energy reserves in the cytoplasm of the bacteria in the form of amorphous water-insoluble inclusion bodies or granules as shown in Figure 2.1A. The PHA granules are also reported to be surrounded by PHA-granules-associated proteins (PGAP) as shown in Figure 2.1B (Cai *et al.*, 2012;

Pfeiffer & Jendrossek, 2014). There are studies showing that almost 90% of the bacterial dry cell weight can comprise of PHAs without causing any harm to the osmotic pressure in the bacterial cells (Fukui & Doi, 1998; Madison & Huisman, 1999). The PHAs accumulated in the bacterial cells can also be utilized by the bacteria through PHA depolymerase which is encoded by the *phaZ* gene that the PHAs accumulated will be degraded into carbon source and be utilized during starvation (Anderson & Dawes, 1990).

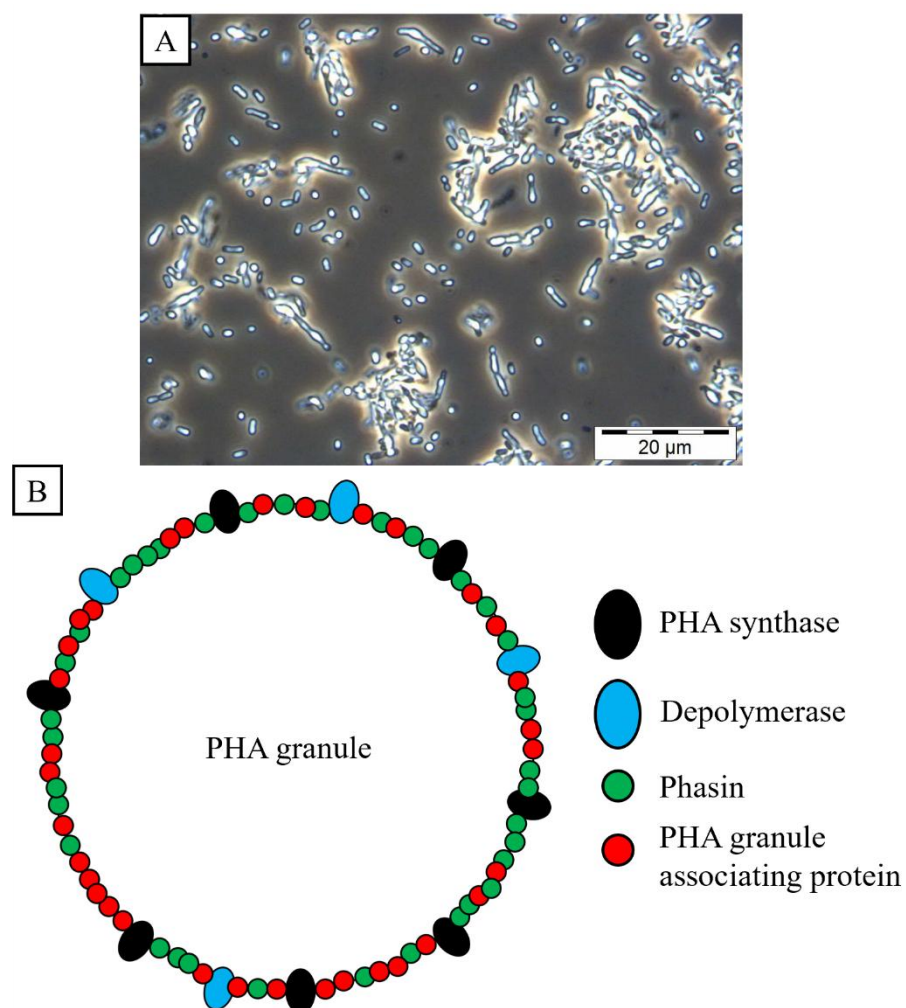


Figure 2.1: PHA accumulated in bacteria cells. (A) Phase contrast light microscopy image of PHA granules (white) in mutant *C. necator* Re2058 harbouring pHTI-CBP-M-CPF4 plasmid cultured in 50 mL minimal medium supplemented with 50 μg/mL kanamycin, 1% (w/v) crude palm kernel oil as a carbon source and 0.054% (w/v) urea as a nitrogen source, shaken at 200 rpm for 48 h in 30 °C. Magnification: 1000×. The PHA accumulated was P(3HB-co-9 mol% 3HHx) and the PHA content was

at 76 wt % of the dry cell weight. (B) Schematic diagram of PHA granule (white) surrounded by proteins. PHA can be surrounded by PHA synthase (PhaC) (black), depolymerase (blue), PHA-granules associated protein (PGAP) (red), and phasin (green).

There are also several categories of PHAs. PHAs can be categorized according to the number of carbon atoms in their respective monomers. The first category is the short-chain length PHA (SCL-PHA) monomers which consist of PHA monomers with 3 to 5 carbon atoms chain long while the second category is the medium-chain length PHA (MCL-PHA) monomers which consist of PHA monomers with 6 to 14 carbon atoms chain length (Sudesh, 2012). SCL-PHAs are known for their stiff, brittle, high crystallinity, high melting temperature, high tensile modulus, and low elongation at break. MCL-PHAs on the other hand have low crystallinity, low melting temperature, and high elongation at break (Yu, 2007). Another category of PHAs is the SCL-MCL-PHA copolymers. They are PHAs consisting of both SCL- and MCL-PHA monomers. They have better thermal and mechanical properties compared to both SCL- and MCL-PHA homopolymers (Kellerhals *et al.*, 2000). Different compositions of the SCL- and MCL-PHA monomers in the SCL-MCL-PHA polymer will give rise to different properties in terms of flexibility and strength (Asrar *et al.*, 2002).

Besides the molar composition of the copolymer, molecular weights also play a role in determining the mechanical strength of the PHAs (Hahn *et al.*, 1994). PHAs with higher molecular weights are known to have better mechanical properties compared to those with lower molecular weights (Aoyagi *et al.*, 2003). The unique feature of PHAs compared to commercial petrochemical plastic is that it is biodegradable and can be degraded into carbon dioxide and water under aerobic conditions and into methane and carbon dioxide under anaerobic conditions by microorganisms (Sudesh *et al.*, 2000). This property of PHA has caught the attention of many researchers and has been

extensively studied to develop strains with increased production of PHA for commercialization purposes.

2.4 Type of PHAs

2.4.1 Poly(3-hydroxybutyrate) [P(3HB)]

Among the reported types of PHAs, P(3HB) has been the subject of substantial research, making it the biopolymer with the best-known characteristic. P(3HB) is a biopolyester having a side chain group at the β -position that is made up of a methyl group and an ester group with four carbon atoms. Figure 2.2 shows the chemical structure of this polymer. The crystallinity of P(3HB) was reported to be between 55% and 80% (Holmes, 1988). This polymer has a glass transition temperature of about 4 °C and a melting temperature that is near 180 °C. P(3HB) homopolymer is also reported to have tensile strength, Young's modulus, and elongation at break of 43 MPa, 3.5 GPa, and 5%, respectively (Sudesh *et al.*, 2000). P(3HB) also has a similar Young's modulus and tensile strength as PP, however, PP has an elongation at break which is 400% greater than P(3HB). P(3HB) is tougher but more brittle than PP. The brittleness of P(3HB) is due to its highly crystalline domains in the form of spherulites. It has been reported that a recombinant *E. coli* harbouring the *phaCI* gene from *C. necator* can accumulate P(3HB) with a weight average molecular weight (M_w) of up to 1.1×10^7 Da (Kusaka *et al.*, 1998). For better mechanical properties, it is preferable to have P(3HB) with higher molecular weights (Aoyagi *et al.*, 2003).

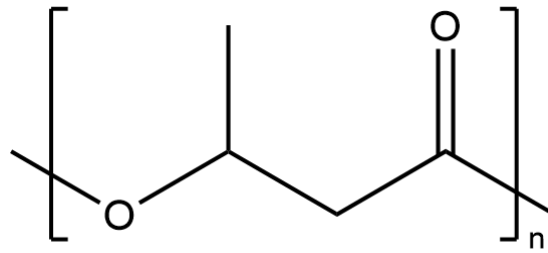


Figure 2.2: Chemical structure of P(3HB). “n” represents the number of repeated units.

2.4.2 Poly(3-hydroxybutyrate-*co*-3-hydroxyhexanoate) [P(3HB-*co*-3HHx)]

P(3HB-*co*-3HHx) is a copolymer made up of two distinct PHA monomers with completely opposite properties, 3HB and 3HHx (an ester group with six carbon atoms and a propyl group as the side chain group at the β -position). 3HB is known for its stiff, brittle, high crystallinity, high melting temperature, high tensile modulus, and low elongation at break while 3HHx is known to have low crystallinity, low melting temperature, and high elongation at break (Yu, 2007). Figure 2.3 shows the copolymer's chemical structure. The crystalline lattices of 3HB and 3HHx monomer units cannot accommodate each other because the 3HHx monomer has a longer alkyl side chain which prevents isodimorphism between the two PHA monomers (Doi *et al.*, 1995). This causes the crystallinity of P(3HB-*co*-3HHx) to reduce from 60 to 18% as the 3HHx monomer composition increased from 0 to 25 mol%. In addition, increasing the 3HHx molar composition of P(3HB-*co*-3HHx) solvent-casted films from 0 to 17 mol% improves the copolymer's elongation at break from 6 to 850% at the cost of lowering its tensile strength from 43 to 20 MPa. As a result, the P(3HB-*co*-3HHx) copolymer becomes softer and more flexible as the 3HHx molar composition increases (Asrar *et al.*, 2002). The increase of 3HHx molar composition from 5 to 25 mol% also greatly reduces the melting temperature from 155 to 52 °C (Doi *et al.*, 1995; Loo *et al.*, 2005). P(3HB-*co*-3HHx) is also known to have similar physical properties as PP and LDPE

(Doi, 1990). Hence, P(3HB-*co*-3HHx) has better properties than P(3HB) in terms of physical properties and ease of processing.

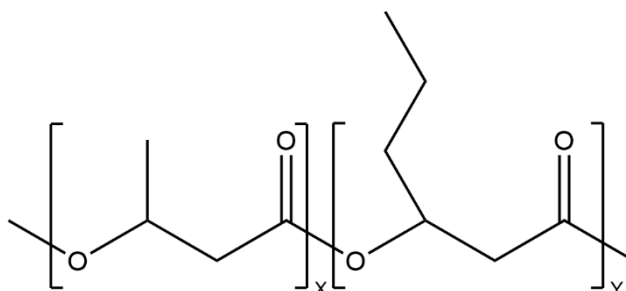


Figure 2.3: Chemical structure of P(3HB-*co*-3HHx). “X” and “Y” represent the number of repeated units.

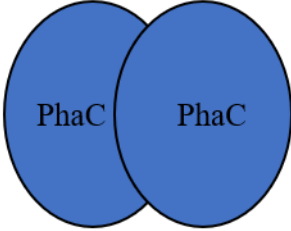
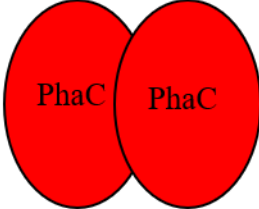
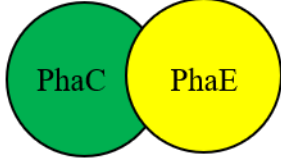
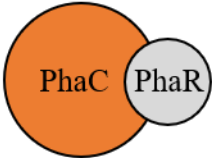
2.5 PHA synthases (PhaCs)

PhaC is the most important enzyme involved in the process of PHA polymerization. The main role of PhaC is to catalyze the polymerization of (*R*)-enantiomer in the form of hydroxyacyl (HA) moiety for instance (*R*)-HA-CoA to PHA polymer chain with the release of CoA (Chek *et al.*, 2017; Kim *et al.*, 2017a; Rehm, 2003; Wittenborn *et al.*, 2016). Due to its ability to polymerize different types of PHA monomers into PHA polymers, PhaCs are known to control the properties of the PHAs produced as different PHA monomers incorporated into the PHA polymer can affect its properties.

PhaCs can also be categorized into 4 different classes, class I, class II, class III, and class IV. Table 2.2 summarizes the different classes of PhaCs. Class I and II PhaCs both contain only one type of subunit, forming a homodimer. The only difference between class I and II PhaCs is class I has substrate specificity towards SCL-PHA monomers while class II has substrate specificities towards MCL-PHA monomers. On the other hand, class III and IV PhaCs are formed by two different subunits hence, forming a heterodimer. Both class III and IV have substrate specificity towards SCL-PHA monomers. The sole difference between class III and IV is that class III PhaC

heterodimer is formed by PhaC and PhaE subunit while class IV is formed by PhaC and PhaR. PhaE and PhaR do not have any similarities to each other (Sudesh, 2012). All PhaC subunits are reported to have a conserved lipase-box-like motif “G-X-[S/C]-X-G” where X can be any amino acid residues and serine is substituted with cysteine in PhaC (Rehm, 2003). Several studies reported that PhaCs have catalytic triads consisting of a nucleophile (cysteine), an acid (aspartic acid), and a base (histidine) (Chek et al., 2017; Jia et al., 2001; Kim et al., 2017a; Wittenborn et al., 2016). These three amino acid residues are reported to be essential for the catalytic activity of the enzyme. This is evident from site-directed mutagenesis and random mutagenesis studies where substitution of any of the amino acid residues forming the catalytic triad causes the PhaC enzyme to lose its activity (Gerngross *et al.*, 1994).

Table 2.2: Different classes of PhaCs based on their subunit compositions and substrate specificities.

Class	Subunits	Substrate
I		SCL-PHA monomers: 3HA-CoA (C3 – C5), 4HA-CoA, 5HA-CoA
II		MCL-PHA monomers: 3HA-CoA (> C5)
III		SCL-PHA monomers: 3HA-CoA (C3 – C5), 4HA-CoA, 5HA-CoA, MCL-PHA monomers: 3HA-CoA (> C5)
IV		SCL-PHA monomers: 3HA-CoA (C3 – C5), 4HA-CoA, 5HA-CoA

Abbreviations: SCL, short-chain-length; MCL, medium-chain-length; 3HA, 3-hydroxyalkanoate; 4HA, 4-hydroxyalkanoate; 5HA, 5-hydroxyalkanoate; C3, PHA monomer with three-carbons length; C5, PHA monomer with five-carbons length; C6 PHA monomer with six-carbons length; C8, PHA monomer with eight-carbons length.

Theoretically, class I PhaCs can only incorporate SCL-PHA monomers into the PHA polymer chain forming SCL-PHA while class II PhaCs can only incorporate

MCL-PHA monomers into the MCL-PHA polymer chain. However, there are always exceptions. For instance, PhaC_{Ac}, PhaC_{Cs}, PhaC from *R. aethiovorans* I24 (PhaC_{Ra}), and PhaC_{BP-M-CPF4} have similarities to class I PhaCs but they can also incorporate 3HHx monomer which is an MCL-PHA monomer into their respective PHA polymer (Bhubalan *et al.*, 2010; Budde *et al.*, 2011; Foong *et al.*, 2018; Fukui & Doi, 1997). This groups them into a special group of class I PhaCs which can incorporate both SCL- and MCL-PHA monomers. Similarly, although PhaC1 and PhaC2 from *Pseudomonas* sp. 61-3 are reported to have similarities to other class II PhaCs, they are also capable of incorporating SCL-PHA monomers into PHA polymer chain, grouping them into a special group of class II PhaCs as well (Matsusaki *et al.*, 1998).

2.5.1 PhaC from mangrove soil metagenome (PhaC_{BP-M-CPF4})

PhaC_{BP-M-CPF4} is class I PhaC first isolated from mangrove soil metagenome of Balik Pulau in Penang, Malaysia. This PhaC is also considered special as this PhaC is one of the handful of PhaCs that belongs to a special class of class I PhaC capable of incorporating SCL-and MCL-PHA monomers into its PHA polymer chain. To date, there is no report on the origin of this PhaC as it is extracted from metagenome data, unlike previously isolated PhaCs like PhaC_{Ac}, PhaC_{Ra}, PhaC_{Cs}, and many more which are from microorganisms. Another interesting fact about this PhaC is that this it is not isolated as a full protein coding sequence due to the absence of a stop codon in the *in silico* generated contig. It is also known for its extremely broad substrate specificity as demonstrated by Foong *et al.* (2018). With the right precursors, it is reported to incorporate up to six different types of PHA monomers, including 3HB, 3HHx, 3HV, 3H4MV, 4HB, and 5HV which has the most substrate specificities of PhaC reported to date. According to previous research, *C. necator*, PHB⁻4 harbouring with PhaC_{BP-M-CPF4} was able to amass up to 62 wt% of P(3HB-co-7mol% 3HHx) from crude palm kernel

oil (CPKO) while in the presence of fructose and sodium hexanoate, the strain can accumulate up to 44 wt% of P(3HB-*co*-18 mol% 3HHx)(Foong *et al.*, 2018). The ability to incorporate a wide range of 3HHx molar composition made this PhaC a good PhaC for P(3HB-*co*-3HHx) production and to be further studied. This is because the 3HHx molar composition in P(3HB-*co*-3HHx) can be adjusted to customize the copolymer for specific applications.

2.6 Metabolic pathway of PHA biosynthesis

There are various pathways for the synthesis of PHA depending on the type of carbon sources fed to the bacteria and the genetics of the bacteria. Different pathways used by the bacteria will end up with different types of PHA polymer produced, provided the PhaC of the bacteria has substrate specificity towards the PHA monomers (Tang *et al.*, 2022). Hence, both pathways and substrate specificity of PhaC must be taken into consideration during strain construction to produce a particular type of PHA polymer.

The most common gene needed for the production of PHA consists of *phaA*, *phaB*, and *phaC* which code for β -ketothiolase, NADPH-dependent acetoacetyl-CoA reductase, and PHA synthase respectively. These three genes are arranged in an operon of *phaC-phaA-phaB* in *Ralstonia eutropha*, currently known as *C. necator* (Anderson & Dawes, 1990; Sudesh *et al.*, 2000). The acetyl-CoA can be from various pathways like glycolysis, β -oxidation, and many more. First, two molecules of acetyl-CoA will undergo condensation which is catalyzed by β -ketothiolase into acetoacetyl-CoA. The acetoacetyl-CoA formed will then be reduced by NADPH-dependent acetoacetyl-CoA reductase forming (*R*)-3-hydroxybutyryl-CoA [(*R*)-3HB-CoA]. Lastly, the

(*R*)-3-hydroxybutyryl-CoA will then be polymerized into chains of PHA by PhaC forming P(3HB) (Figure 2.4 black box).

Besides P(3HB), other types of PHA copolymers can be formed. For instances P(3HB-*co*-3HHx), poly(3-hydroxybutyrate-*co*-3-hydroxyvalerate), [P(3HB-*co*-3HV)], poly(3-hydroxybutyrate-*co*-4-hydroxybutyrate), [P(3HB-*co*-4HB)] and many more. When oil is fed as the carbon source to the bacteria for PHA production, oil or triacylglyceride will be hydrolyzed by lipase enzymes into glycerol and free fatty acids. The fatty acid will then be converted to acyl-CoA by acyl-CoA synthetase (FadD) followed by oxidation by acyl-CoA dehydrogenase (FadE) resulting in *trans*-2-enoyl-CoA. The resulting *trans*-2-enoyl-CoA will then be hydrated into (*S*)-3-hydroxyacyl-CoA by *trans*-2-enoyl-CoA hydratase (FadB) followed by oxidation into 3-ketoacyl-CoA by 3-hydroxyacyl-CoA dehydrogenase (Had). 3-ketoacyl-CoA will then be converted back to acyl-CoA but with two carbons less due to the release of one acetyl-CoA by 3-ketoacyl-CoA thiolase (FadA). The acetyl-CoA release can be utilized by PhaA, PhaB, and PhaC as described in the previous discussion. Rather than converting the *trans*-2-enoyl-CoA to (*S*)-3-hydroxyacyl-CoA by *trans*-2-enoyl-CoA hydratase (FadB), the *trans*-2-enoyl-CoA can also be converted to also be converted directly by (*R*)-*trans*-2-enoyl-CoA hydratase (PhaJ) to (*R*)-3-hydroxyacyl-CoA. This (*R*)-3-hydroxyacyl-CoA can be incorporated into PHA polymer by PhaC. An example of a type of PHA incorporated this way is mostly PHA with MCL-PHA monomers like P(3HB-*co*-3HHx) (Figure 2.4 red box) (Tsuge, 2002).

As discussed above, when sugar is fed as the carbon source for the bacteria, the sugar will be converted to acetyl-CoA and subsequently be converted to PHA by PhaA, PhaB, and PhaC forming P(3HB) homopolymer. There is an engineered pathway that involves the formation of P(3HB-*co*-3HHx) using sugar through a synthetic pathway.

When sugar is fed as a carbon source, sugar will be converted to acetyl-CoA through glycolysis and pyruvate dehydrogenase. The acetyl-CoA will also be converted into acetoacetyl-CoA by PhaA, but unlike in the previous discussion, acetoacetyl-CoA will be reduced to (*S*)-3-hydroxybutyryl-CoA [(*S*)-3HB-CoA] by (*S*)-3HB-CoA dehydrogenase (Had). (*S*)-3HB-CoA will then be converted to crotonoyl-CoA by crotonase (Crt2) followed by conversion to (*R*)-3HB-CoA by PhaJ or butyryl-CoA by crotonoyl-CoA reductase (Ccr). The (*R*)-3HB-CoA will be incorporated into PHA as 3HB while the butyryl-CoA will be further converted to 3-oxohexanoyl-CoA followed by reduction to (*S*)-3HHx-CoA by Had. The (*S*)-3HHx-CoA will be converted to 2-hexenoyl-CoA by Crt2 and followed by hydration to (*R*)-3HHx-CoA by PhaJ. The (*R*)-3HHx-CoA will then be incorporated as 3HHx in PHA polymer by PhaC (Figure 2.4 blue box) (Zhang *et al.*, 2019).

When odd-chain organic acids are added to the bacteria as a carbon source, another type of PHA, P(3HB-*co*-3HV) will be accumulated within the bacteria. The organic acid will be metabolized leading to the formation of propionyl-CoA. Condensation of propionyl-CoA and acetyl-CoA by β -ketothiolase (BktB) will lead to the formation of ketovaleryl-CoA which will subsequently be reduced by PhaB into (*R*)-3-hydroxyvaleryl-CoA. The (*R*)-3-hydroxyvaleryl-CoA will then be incorporated into PHA polymer while 3HB will arise from acetyl-CoA giving rise to P(3HB-*co*-3HV) (Figure 2.4 green box) (Steinbüchel & Lütke-Eversloh, 2003).

As for P(3HB-*co*-4HB), production of such PHA can be produced by bacteria expressing succinic semialdehyde dehydrogenase, 4-hydroxybutyrate dehydrogenase, and succinyl-CoA:CoA transferase. As discussed above, the 3HB-CoA will be formed by the acetyl-CoA while succinyl-CoA, an intermediate in the tricarboxylic acid (TCA) or citric acid cycle will be converted to 4HB-CoA. First, succinyl-CoA will be oxidized

to succinic semialdehyde by succinic semialdehyde dehydrogenase followed by another oxidation by 4-hydroxybutyrate dehydrogenase to form 4-hydroxybutyrate. The 4-hydroxybutyrate will then be converted to (*R*)-4-hydroxybutyrate-CoA by succinyl-CoA:CoA transferase to be incorporated by PhaC forming P(3HB-*co*-4HB) (Figure 2.4 purple box) (Lütke-Eversloh & Steinbüchel, 1999; Valentin *et al.*, 1995).

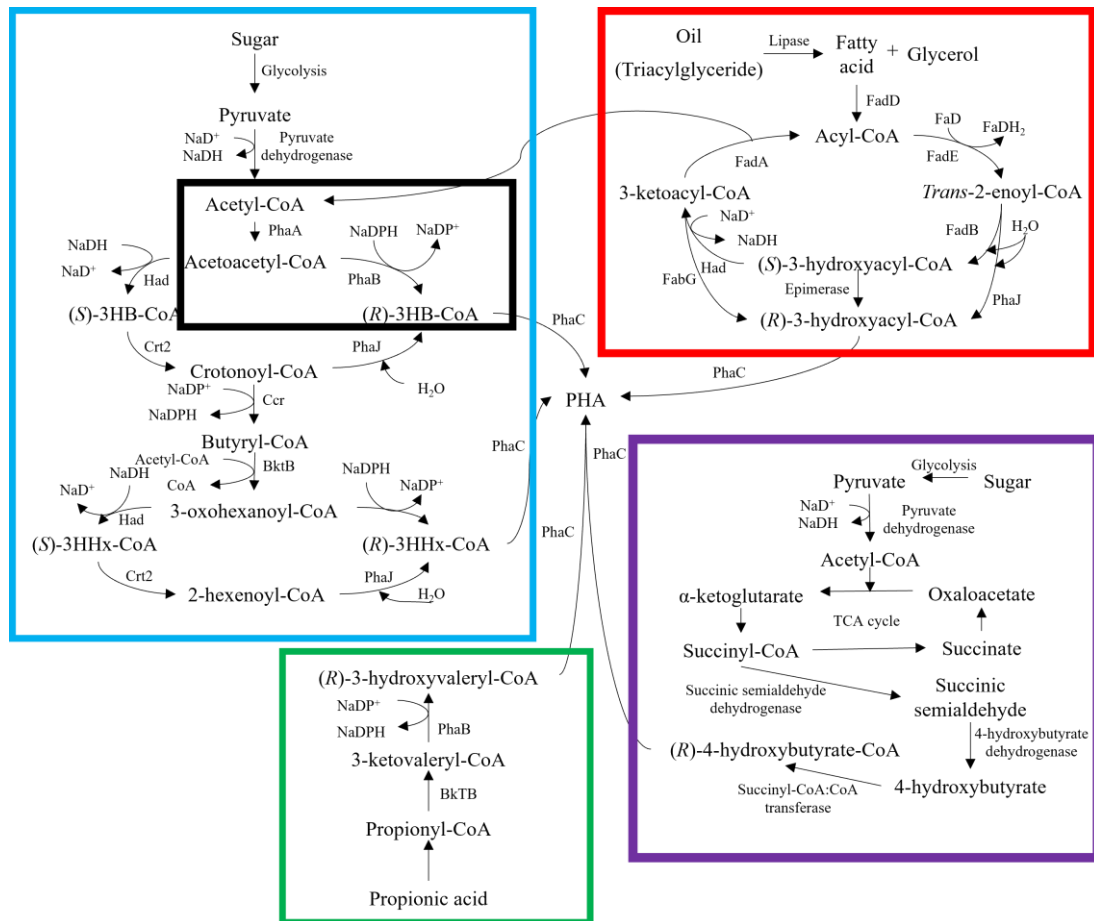


Figure 2.4: Metabolic pathway of PHA biosynthesis. The black box, red box, blue box, green box, and purple box represent the pathway used by bacteria for the production of P(3HB), P(3HB-*co*-3HHx) using oil, P(3HB-*co*-3HHx) using sugar, P(3HB-*co*-3HV), and P(3HB-*co*-4HB) respectively.

2.7 3-D structure of PHA synthase (PhaC)

To date, there are only two crystal structures of PhaCs successfully obtained through protein X-ray crystallography. The first reported crystal structure of PhaC is PhaC_{Cn} with a resolution of 1.8 Å (Chek *et al.*, 2017; Kim *et al.*, 2017a). Another crystal

structure of PhaC is PhaC_{Cs} with a resolution of 1.48 Å (Chek *et al.*, 2017). Generally, the structure of PhaCs can be divided into two distinct domains, the N- and C-terminal. Both structures are reported to exist as a dimer and form the α/β hydrolase fold with α/β core and CAP subdomain. Based on the reported crystal structure, the active site of PhaC_{Cn} consisted of Cys319, Asp480, and His508 while the active site of PhaC_{Cs} consisted of Cys291, Asp447, and His477 (Chek *et al.*, 2017; Kim *et al.*, 2017a; Wittenborn *et al.*, 2016). However, the crystal structure of PhaC_{Cs} reported is in closed form, distinctly from the crystal structure of PhaC_{Cn} reported by Kim *et al.* (2017), which had a partially open form while maintaining a narrow substrate access channel to the active site. The structure of PhaC_{Cs} was also reported to form a face-to-face dimer mediated by the CAP subdomains. The arrangement of the dimer was also found to be distinct from the crystal structure of PhaC_{Cn}. It was also suggested that the CAP subdomain should undergo conformational changes during catalytic activity, which involved rearrangement of the dimer to allow the entry of substrate and product egress after production formation (Chek *et al.*, 2017). Subsequently, there was a report on the crystal structure of PhaC_{Cs} which had a CoA molecule binding to the PhaC_{Cs}, elucidating how the substrate would bind to the PhaC during polymerization. Surprisingly, the previously reported histidine residue that formed the catalytic triad is folded out from the active site when the substrate is binding to the PhaC. This suggests that histidine may not be involved with the polymerization of PHA monomers but rather only acts as an activator to activate the cysteine residue for nucleophilic attack on the PHA monomer substrates (Chek *et al.*, 2020).

To date, there are two proposed catalytic mechanisms for PHA synthesis. One is the non-processive ping-pong model, and another is the processive model. The non-processive ping-pong model requires two active sites of the dimeric-structured

PhaC for the PHA elongation step wherein chain transfer will take place between the two cysteine residues across the dimer interface (Kim *et al.*, 2017a). On the contrary, only one single active site is needed for the elongation step of the processive model (Chek *et al.*, 2017; Wittenborn *et al.*, 2016). To date, the more suitable catalytic mechanism for PHA synthesis will be the processive model which requires only one active site. This is because, in the non-processive ping-pong model, the distance between the two active sites of the dimeric-structured PhaC is too far apart for the polymer chain transfer to occur between one another (Chek *et al.*, 2017). Another evidence is that the structure of PhaC_{Cs} bound to a CoA molecule showed an asymmetric open-closed conformation where one subunit is in the opened conformation while another is in the closed conformation.

In general, the catalytic triad of cysteine, aspartic acid, and histidine makes up the PhaCs' catalytic mechanism. Other systems that use this catalytic triad include lipases, esterases, and serine proteases. The histidine residue will activate the cysteine residue which acts as a nucleophile. During the catalytic cycle of PhaCs, the activated cysteine residue will execute a nucleophilic attack on the thioester bond of an acyl-CoA, such as 3HB-CoA. This releases the CoA molecule from the 3HB-CoA, resulting in the formation of a covalently bound intermediate, Cys-3HB, and the CoA molecule will leave the binding pocket. Histidine or aspartic acid will then activate the second incoming substrate, 3HB-CoA, in the elongation phase by deprotonating the hydroxyl group of the incoming 3HB-CoA. The Cys-3HB thioester bond will then be attacked by the activated 3HB-CoA substrate, generating the noncovalent intermediate (3HB)₂-CoA (Chek *et al.*, 2017; Kim *et al.*, 2017a; Wittenborn *et al.*, 2016). Due to the reported asymmetric open-closed structure of PhaC_{Cs} bound to CoA molecule, it is shown that it is aspartic acid residue and not histidine residue that activates the second incoming

3HB-CoA molecule during PHA elongation step because the histidine residue is folded out from its catalytic pocket (Chek *et al.*, 2020).

2.8 N-terminal region of PHA synthase (PhaC)

To date, there is no report on the crystal structure of the full-length PhaC. The two crystal structures of PhaC reported were N-terminal truncated. Hence, the structural information and specific function of the N-terminal domain remains unknown, and crystallization attempts to view this region's structure were unsuccessful. This is because the N-terminal region of PhaC was reported to be flexible which hinders the crystallization process of the protein crystal (Chek *et al.*, 2017). To elucidate the crystal structure of full-length PhaC, Kim *et al.* (2017b) inserted a point mutation, R192A (substitution of arginine at position 192 with alanine) because proteolytic cleavage occurred at R192 during the crystallization process. However, even after numerous attempts, the diffraction of the resulting protein crystals remained bad and could not be improved (Kim *et al.*, 2017b).

Previously, Rehm (2003) postulated that the N-terminal domain of PhaC consists of the first 100 amino acids due to the region's high degree of diversity, which was demonstrated through multiple sequence alignment studies (Rehm, 2003). However, based on the reported PhaC_{Cn} and PhaC_{Cs} crystal structures, it is possible that the N-terminal domains of various PhaCs could have different lengths. Given that the C-terminal catalytic domain of PhaC_{Cn} and PhaC_{Cs} remained stable and crystallizable in the absence of the N-terminal domain (Chek *et al.*, 2017; Kim *et al.*, 2017a; Wittenborn *et al.*, 2016). Hence, it can be hypothesized that the N-terminal domains of PhaC_{Cn} and PhaC_{Cs} are the first 200 and 174 amino acids, respectively.